Trigonometry-Based Numerical Method to Compute Nonlinear Magnetic Characteristics in Switched Reluctance Motors

X. D. Xue, K. W. E. Cheng, S. L. Ho, and K. F. Kwok

Department of Electrical Engineering, The Hong Kong Polytechnic University, Hong Kong, China

Based on two-dimensional (2-D) trigonometry, a new numerical method is presented to compute the nonlinear magnetic and electromagnetic torque characteristics in switched reluctance motors (SRMs). In the proposed method, the mathematical model is composed of the 2-D truncated Fourier series. The coefficients can be determined from a small amount of given magnetic or torque data acquired by experiment or finite-element (FE) analysis. The computed and experimental results demonstrate that the proposed method can be used to precisely compute the nonlinear magnetic and torque characteristics in SRMs. Hence, this paper provides a valuable approach for performance prediction, design, simulation, and control of SRMs.

***Index Terms*—Model, nonlinear magnetics, switched reluctance motors, torque.**

I. Introduction

SWITCHED reluctance motors (SRMs) usually run with heavy magnetic saturation in order to produce a large ratio of torque to mass. Indeed, magnetic saturation plays a key role in underpinning the high performance of SRMs. However, magnetic saturation in SRMs results in high nonlinearities in their magnetic and torque characteristics, thereby making the analysis and control of SRM drives very complicated. Thus, an accurate algorithm to describe the nonlinear magnetic characteristics of SRMs is extremely useful for performance prediction, simulation, optimization, sensorless and torque controls of SRM drives.

Methods to describe the magnetic nonlinearities in SRMs mainly include four approaches, which are, namely: 1) interpolation methods [1] in which the given nonlinear magnetic data of SRMs are stored in tabular form and the phase flux linkage or inductance is interpolated using appropriate piecewise interpolation methods; 2) analytical methods [2] in which proper analytical expressions are derived to characterize the nonlinearities of the phase flux linkage or inductance characteristics with respect to the phase current and the rotor position; 3) ANN models [3] are developed to describe the nonlinear magnetic characteristics of SRMs, however these models need to be trained by a large number of given discrete magnetic data before they can be used to compute the magnetic characteristics at any current and rotor position; and 4) equivalent magnetic circuit methods [4] in which analytical expressions, which are based on equivalent magnetic circuits and permeance, are used to compute the magnetic characteristics of SRMs.

Previous methods have either fast computation or good accuracy, but not both. This paper presents a new numerical method to quickly and accurately compute the nonlinear magnetic and electromagnetic torque characteristics in SRMs. The proposed method is based on the 2-D truncated Fourier series. Two types of computation errors are utilized to evaluate the accuracy of the proposed method. Excellent agreements between the experimental and computed results for the flux linkage or torque characteristics in SRMs are a good validation of the proposed method.

The organization of this paper is as follows. In Section II, the model and computation of the Fourier coefficients are presented. Two application cases are shown in Section III. Finally, the conclusions are drawn in Section IV.

II. Proposed Numerical Method

A. Model

Both the flux linkage and the electromagnetic torque are nonlinear functions of rotor position and current in SRMs. The mathematical model used by the proposed method consists of the 2-D truncated Fourier series and can be expressed by

$$F(\theta,i)=\sum_{p_\theta=-M_\theta}^{M_\theta}\sum_{p_i=-M_i}^{M_i}c_{p_\theta,p_i}\exp(-j(p_\theta k_\theta\hat{\theta}+p_i k_i\hat{i})) \tag{1}$$

where F may denote the flux linkage, inductance, or torque; θ denotes the rotor position confined in $\theta_{\min}<\theta<\theta_{\max}$; i denotes the current confined in $i_{\min}<i<i_{\max}$; M_θ and M_i are two specified truncation levels; j is the imaginary unity; c_{p_θ,p_i} are complex Fourier coefficients; and

$$\begin{aligned}\hat{\theta}&=\theta-\theta_{\min}\\ \hat{i}&=i-i_{\min}\\ k_\theta&=2\pi/L_\theta\\ k_i&=2\pi/L_i\\ L_\theta&=\theta_{\max}-\theta_{\min}\\ L_i&=i_{\max}-i_{\min}.\end{aligned} \tag{2}$$

The Euler formula is given by

$$e^{\pm jz}=\cos z\pm j\sin z. \tag{3}$$

Digital Object Identifier 10.1109/TMAG.2007.892619

To ensure that the right-hand side of (1) is a real number, it is clear that the coefficients c_{p_θ,p_i} must satisfy

$$c_{-p_\theta,-p_i} = c^*_{p_\theta,p_i} \tag{4}$$

where an asterisk signifies the complex conjugate.

Using the orthogonal properties of the trigonometric functions, the Fourier coefficients c_{p_θ,p_i} are determined by [5]

$$c_{p_\theta,p_i} = \frac{1}{L_\theta L_i}\int_{\theta_{\min}}^{\theta_{\max}}\int_{i_{\min}}^{i_{\max}} f(\theta,i)\exp(j(p_\theta k_\theta\hat{\theta}+p_i k_i\hat{i}))didd\theta \tag{5}$$

where $f(\theta,i)$ are the given values that may be the flux linkage, inductance, or torque.

B. Computation of c_{p_θ,p_i}

Equations (5) and (4) may be computed by numerical integration. Thus, the Fourier coefficients will depend on the selected integration rule or quadrature. However the above truncated Fourier series will not generally be an interpolating function, that is, it will not necessarily interpolate through the data points. To solve (5), the interval L_θ is divided into N_θ subintervals separated by $N_\theta+1$ grid lines $\theta_l = \theta_{\min}+(l-1)h_\theta, l = 1,\ldots,N_\theta+1$, where $h_\theta = L_\theta/N_\theta, \theta_1 = \theta_{\min}, \theta_{N\theta+1} = \theta_{\max}$. Similarly, the interval L_i is divided into N_i subintervals separated by the N_i+1 grid lines $i_k = i_{\min}+(k-1)h_i, k = 1,\ldots,N_i+1$, where $h_i = L_i/N_i, i_1 = i_{\min}, i_{Ni+1} = i_{\max}$.

Using the trapezoidal integration rule to evaluate the complex Fourier integral in (5), one obtains [5]

$$c_{p_\theta,p_i} = \frac{C_{N_\theta}}{N_\theta N_i}\left(\frac{1}{2}q_1+\omega_\theta^{p_\theta}q_2+\cdots+\omega_\theta^{p_\theta(N_\theta-1)}q_{N_\theta}+\frac{1}{2}q_{N_\theta+1}\right) \tag{6}$$

where

$$q_s(p_i) = C_{N_i}\left(\frac{1}{2}f_{s,1}+\omega_i^{p_i}f_{s,2}+\cdots+\omega_i^{p_i(N_i-1)}f_{s,N_i}+\frac{1}{2}f_{s,N_i+1}\right) \tag{7}$$

$$f_{s,r} = f(\theta_s,i_r) \tag{8}$$

$$\omega_\theta = \exp(jk_\theta h_\theta)$$

$$\omega_i = \exp(jk_i h_i). \tag{9}$$

It should be noted that $\omega_\theta^{N_\theta} = 1$ and $\omega_i^{N_i} = 1$.

The values of $M_\theta, M_i, C_{N\theta}$, and C_{Ni} are determined according to the following rules. a) When the number of interval N_θ is odd, (1) is truncated at the value $M_\theta = (N_\theta-1)/2$. When N_θ is even, it is truncated at the value $M_\theta = N_\theta/2$. Similar truncation levels pertain to M_i. b) When N_i is even, C_{Ni} is equal to $1/2$ for $p_i = -M_i$ and M_i, for s from (7) $= 1,\ldots,N_\theta+1$. Otherwise, C_{Ni} is equal to 1. c) When N_θ is even, $C_{N\theta}$ is $1/2$ for $p_\theta = -M_\theta$ and M_θ for $p_i = -M_i,\ldots,M_i$. Otherwise, $C_{N\theta}$ is 1 [5].

Because the right-hand side of (1) is a real number, it is necessary to derive the real term of the expression.

First, substituting (9) into (7) gives

$$q_s(p_i) = C_{N_i}\left[\frac{1}{2}(f_{s,1}+f_{s,N_i+1})+\sum_{r=2}^{N_i}f_{s,r}e^{jk_ih_ip_i(r-1)}\right]. \tag{10}$$

Next, substituting (10) into (6) results in

$$\begin{aligned}c_{p_\theta,p_i} = \frac{C_{N_\theta}C_{N_i}}{N_\theta N_i}\Bigg\{&\left[\frac{1}{4}(f_{1,1}+f_{1,N_i+1}+f_{N_\theta+1,1}+f_{N_\theta+1,N_i+1})\right]\\&+\left[\frac{1}{2}\sum_{r=2}^{N_i}(f_{1,r}+f_{N_\theta+1,r})e^{jk_ih_ip_i(r-1)}\right]\\&+\left[\frac{1}{2}\sum_{s=2}^{N_\theta}(f_{s,1}+f_{s,N_i+1})e^{jk_\theta h_\theta p_\theta(s-1)}\right]\\&+\left[\sum_{s=2}^{N_\theta}\sum_{r=2}^{N_i}f_{s,r}e^{jk_ih_ip_i(r-1)}e^{jk_\theta h_\theta p_\theta(s-1)}\right]\Bigg\}.\end{aligned} \tag{11}$$

Then, substituting (3) into (11), the computations of the Fourier coefficients c_{p_θ,p_i} can be given by

$$\begin{aligned}c_{p_\theta,p_i} = \frac{C_{N_\theta}C_{N_i}}{N_\theta N_i}\Bigg\{&\frac{1}{4}(f_{1,1}+f_{1,N_i+1}+f_{N_\theta+1,1}+f_{N_\theta+1,N_i+1})\\&+\frac{1}{2}\sum_{r=2}^{N_i}(f_{1,r}+f_{N_\theta+1,r})[\cos(k_ih_ip_i(r-1))\\&+j\sin(k_ih_ip_i(r-1))]+\frac{1}{2}\sum_{s=2}^{N_\theta}(f_{s,1}+f_{s,N_i+1})\\&\times[\cos(k_\theta h_\theta p_\theta(s-1))+j\sin(k_\theta h_\theta p_\theta(s-1))]\\&+\sum_{s=2}^{N_\theta}\sum_{r=2}^{N_i}f_{s,r}[\cos(k_ih_ip_i(r-1)+k_\theta h_\theta p_\theta(s-1))\\&+j\sin(k_ih_ip_i(r-1)+k_\theta h_\theta p_\theta(s-1))]\Bigg\}.\end{aligned} \tag{12}$$

Finally, the real part of c_{p_θ,p_i} can be expressed by

$$\begin{aligned}\Re(c_{p_\theta,p_i}) = \frac{C_{N_\theta}C_{N_i}}{N_\theta N_i}\Bigg\{&\frac{1}{4}(f_{1,1}+f_{1,N_i+1}+f_{N_\theta+1,1}\\&+f_{N_\theta+1,N_i+1})+\frac{1}{2}\sum_{r=2}^{N_i}(f_{1,r}+f_{N_\theta+1,r})\cos[k_ih_ip_i(r-1)]\\&+\frac{1}{2}\sum_{s=2}^{N_\theta}(f_{s,1}+f_{s,N_i+1})\cos[k_\theta h_\theta p_\theta(s-1)]\\&+\sum_{s=2}^{N_\theta}\sum_{r=2}^{N_i}f_{s,r}\cos[k_ih_ip_i(r-1)+k_\theta h_\theta p_\theta(s-1)]\Bigg\}.\end{aligned} \tag{13}$$

The imaginary part of c_{p_θ,p_i} can be computed from

$$\begin{aligned}\Im(c_{p_\theta,p_i}) = \frac{C_{N_\theta}C_{N_i}}{N_\theta N_i}\Bigg\{&\frac{1}{2}\sum_{r=2}^{N_i}(f_{1,r}+f_{N_\theta+1,r})\sin[k_ih_ip_i(r-1)]\\&+\frac{1}{2}\sum_{s=2}^{N_\theta}(f_{s,1}+f_{s,N_i+1})\sin[k_\theta h_\theta p_\theta(s-1)]\\&+\sum_{s=2}^{N_\theta}\sum_{r=2}^{N_i}f_{s,r}\sin[k_ih_ip_i(r-1)+k_\theta h_\theta p_\theta(s-1)]\Bigg\}.\end{aligned} \tag{14}$$

TABLE I
COMPUTATION ERRORS FOR THE FLUX LINKAGE CHARACTERISTICS

Case	SSE (Wb^2)	MAVE (Wb)
Fitting points	1.35×10^{-17} %	6.39×10^{-9} %
Fig. 1	3.1×10^{-2} %	3.53×10^{-1} %
Fig. 2	2.33×10^{-2} %	4.59×10^{-1} %

Hence, substituting (13) and (14) into (1), the computations of the flux linkage, inductance, or torque with respect to the rotor position and the current are determined by

$$F(\theta,i)=\sum_{p_\theta=-M_\theta}^{M_\theta}\sum_{p_i=-M_i}^{M_i}[\Re(c_{p_\theta,p_i})\cos(p_\theta k_\theta\hat{\theta}+p_i k_i\hat{i}) +\Im(c_{p_\theta,p_i})\sin(p_\theta k_\theta\hat{\theta}+p_i k_i\hat{i})]. \quad (15)$$

III. APPLICATIONS

The proposed numerical method is used to compute the nonlinear magnetic and torque characteristics of a four-phase SRM. The rotor position period is 60° for the four-phase SRM. Furthermore, the magnetic characteristics are symmetrical about the position of 30° and the torque characteristics are antisymmetrical about the position of 30°, within a position period. Hence, the domain of the rotor position may be defined from 0° to 30°. For the prototype, the domain of the current is defined from 0 to 12 A. The rotor position is equal to 0° when the stator pole is just unaligned with the rotor pole.

Two types of the computation errors are used to evaluate the proposed numerical method. One is the square sum of errors (SSE) and the other is the maximum absolute value of errors (MAVE). They are defined by, respectively

$$\mathrm{SSE}=\sum_{k=1}^{N_p}\sum_{l=1}^{N_c}(F_{k,l}-f_{k,l})^2 \quad (16)$$

and

$$\mathrm{MAVE}=\max_{\substack{0\le k\le N_p\\0\le l\le N_c}}|F_{k,l}-f_{k,l}| \quad (17)$$

where $F_{k,l}$ represents the computed values by using the proposed method; $f_{k,l}$ represents the given values; N_p is the number of the rotor positions; and N_c is the number of the currents.

A. Computation of Nonlinear Flux Linkage Characteristics

The real and imaginary parts of the coefficients c_{p_θ,p_i} are computed from the given data of the flux linkage with respect to the rotor position and current. The computation errors at the fitting points are shown in Table I. The proposed numerical method is used to compute the flux linkage at any position and current. Fig. 1 illustrates the computed and experimental results of the flux linkage versus the rotor position at a set of currents. The computed and experimental results of the flux linkage versus the current at a set of rotor positions can be found in Fig. 2. Two types of computation errors corresponding to Figs. 1 and 2 are given in Table I.

It can be found from Figs. 1 and 2 that the computed flux linkage values using the proposed method are very consistent with the experimental data. Moreover, it also can be seen from

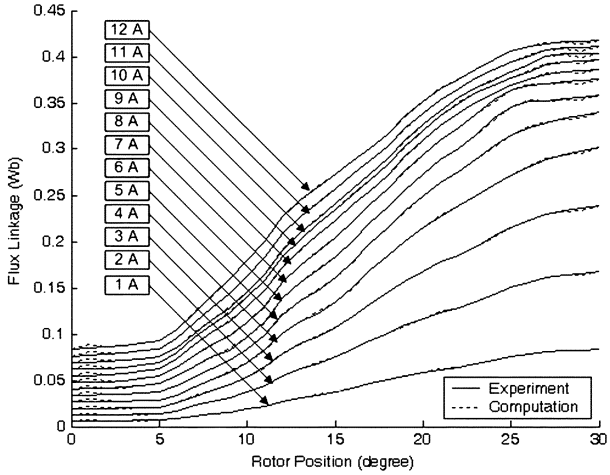

Fig. 1. Flux linkage versus the rotor position.

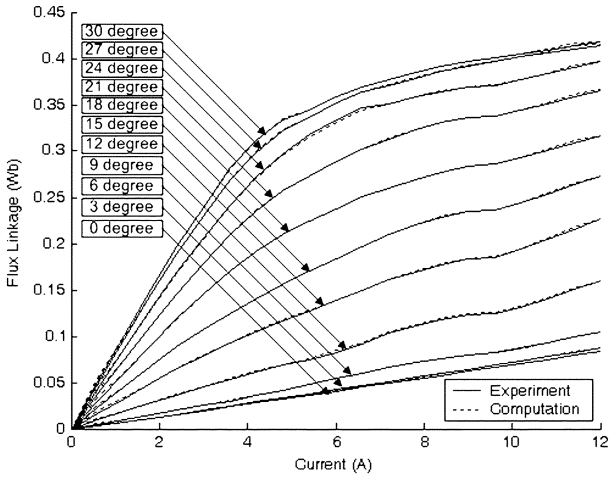

Fig. 2. Flux linkage versus the current.

Table I that SSE and MAVE at either the fitting or nonfitting points, particularly at the fitting points, are very small. These serve as a good validation of the presented equations and demonstrate that the proposed method can be used to accurately compute the nonlinear flux linkage characteristics with respect to the rotor position and current in SRMs.

B. Computation of Nonlinear Torque Characteristics

Torque characteristics in SRMs are highly nonlinear. Furthermore, the torque computation is crucial for the control of torque ripple minimization and direct torque control. The proposed method can be utilized to compute the torque characteristics in which the Fourier coefficients are determined from a limited number of given static torque data. Table II shows the computation errors at the fitting points. Fig. 3 depicts the computed results and the given data versus the rotor position at a group of currents.

It can be observed from Fig. 3 that the computed torque values are in good agreement with the given data. Furthermore, Table II also indicates the computation errors at both the fitting points and at those arbitrary points as shown in Fig. 3. As similar to the computation of flux linkage characteristics, the computation errors at the fitting points are extremely small and the computation errors at arbitrary points are also remarkably small. These

TABLE II
COMPUTATION ERRORS FOR TORQUE CHARACTERISTICS

Case	SSE (Wb^2)	MAVE (Wb)
Fitting points	3.45×10^{-15} %	6.98×10^{-8} %
Fig. 3	5.38 %	8.09 %

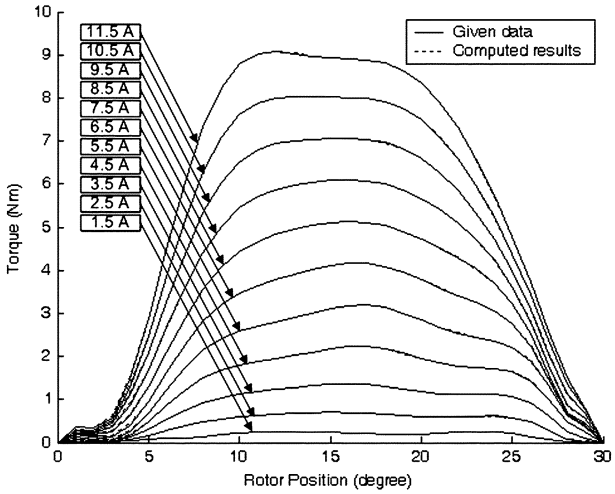

Fig. 3. Computed and given static torque characteristics.

validate again the presented equations and demonstrate that the proposed method can also be used to accurately compute the nonlinear torque characteristics in the SRM.

IV. CONCLUSION

Based on trigonometry, this paper has presented a new numerical method to compute the nonlinear magnetic and torque characteristics in SRMs. Such a method is composed of the 2-D truncated Fourier series. The proposed 2-D Fourier series can be used to analytically compute the nonlinear magnetic and torque characteristics in SRMs. On the other hand, the coefficients in the Fourier series have to be computed by using the proposed numerical method. In terms of methodology, hence, the proposed method may be regarded as a hybrid approach in the computation of the magnetic characteristics in SRMs.

The proposed method has been applied successfully to compute the flux linkage and static torque characteristics with respect to the rotor position and current in the SRM being studied. It can be shown that the computed results, irrespective of whether they are the flux linkage characteristics or torque characteristics, using the proposed method are very consistent with the given data. Moreover, the computation errors at the fitting points are extremely small and the computation errors at arbitrary positions and currents are also remarkably small. All of these therefore demonstrate that the proposed method can be used to precisely compute the nonlinear flux linkage and torque characteristics in SRMs.

The salient advantage of the proposed method is its excellent accuracy. It has: 1) very fast computation time when compared to that of previous interpolation methods and 2) very good accuracy when compared to previous analytical methods, ANN methods, and equivalent magnetic circuit methods. Therefore, this paper provides an effective and precise approach to compute the nonlinear magnetic or torque characteristics for performance prediction, performance optimization, simulation, sensorless control, and torque control of SRMs.

ACKNOWLEDGMENT

This work was supported in part by the Research Committee of The Hong Kong Polytechnic University (Project code: G-YX52).

REFERENCES

[1] X. D. Xue, K. W. E. Cheng, and S. L. Ho, "Simulation of switched reluctance motor drives using two-dimensional bicubic spline," *IEEE Trans. Energy Convers.*, vol. 17, no. 4, pp. 471–477, Dec. 2002.

[2] X. D. Xue, K. W. E. Cheng, and S. L. Ho, "A self-training numerical method to calculate the magnetic characteristics for switched reluctance motor drives," *IEEE Trans. Magn.*, vol. 40, no. 2, pp. 734–737, Mar. 2004.

[3] A. A. Arkadan, P. Du, M. Sidani, and M. Bouji, "Performance prediction of SRM drives systems under normal and fault operating conditions using GA-based ANN method," *IEEE Trans. Magn.*, vol. 36, no. 4, pp. 1945–1949, Jul. 2000.

[4] V. Vujicic and N. Vukosavic, "A simple nonlinear model of the switched reluctance motor," *IEEE Trans. Energy Convers.*, vol. 15, no. 4, pp. 395–400, Dec. 2000.

[5] C. Pozrikidis, *Numerical Computation in Science and Engineering*. Oxford, U.K.: Oxford Univ. Press, 1998.

Manuscript received April 24, 2006 (e-mail: eeecheng@polyu.edu.hk).